Induction of DNA damage by heavy ions measured by atomic force microscopy

2005 J. Phys.: Condens. Matter 17 S1443

(http://iopscience.iop.org/0953-8984/17/18/002)

INSTITUTE OF PHYSICS PUBLISHING JOURNAL OF PHYSICS: CONDENSED MATTER

J. Phys.: Condens. Matter **17** (2005) S1443–S1446 doi:10.1088/0953-8984/17/18/002

Induction of DNA damage by heavy ions measured by atomic force microscopy

K Psonka[1,2], **S Brons**[2], **M Heiss**[2], **E Gudowska-Nowak**[1,2] **and G Taucher-Scholz**[2]

[1] Marian Smoluchowski Institute of Physics, Jagiellonian University, Reymonta 4, Krakow, Poland
[2] Biophysics Department, Gesellschaft für Schwerionenforschung (GSI), Planckstrasse 1, Darmstadt, Germany

E-mail: psonka@th.if.uj.edu.pl

Received 4 October 2004, in final form 20 December 2004
Published 22 April 2005
Online at stacks.iop.org/JPhysCM/17/S1443

Abstract

According to the experimental evidence damage induced by densely ionizing radiation in chromosomes and DNA molecules is distributed in the form of clusters. The most critical type of DNA damage is double-strand breaks (DSBs) which are formed when breaks occur in both DNA strands and are directly opposite or separated by only a few base pairs. This paper reports on the direct visualization of DSBs induced in a plasmid DNA molecule by ionizing radiation and the measurement of produced DNA fragments by use of atomic force microscopy (AFM). Our results show an influence of radiation quality on the DSB production.

1. Introduction

DNA double-strand breaks (DSBs) are generally considered to be at the origin of the biological damage induced by ionizing radiation [1]. In particular, misrepaired or unrepaired DSBs have been implicated as lesions resulting in cell killing, mutations or carcinogenesis. The molecular nature of DNA damage and the production of DSBs are expected to be determined by the spatial distribution of the ionization events, which itself depends on the physical properties of energy deposition and the chemical environment of the DNA [2]. Radiation-quality-dependent differences in the response to ionizing radiation are considered to result from the induction of more severe and less repairable lesions by high linear energy transfer (LET) radiation as compared to low LET radiation, being more likely to create pairs of DSBs in a single ionization event.

Within an individual ion track, the energy deposited within the medium decreases steeply with the distance from the particle trajectory up to a maximum distance that depends on the particle energy. Therefore very high local doses are deposited in the track centre, whereas large

regions of negligible dose deposition occur between the individual tracks. In consequence, a high density of biological damage is expected at the sites close to the particle trajectory. This localization effect is responsible for DSBs clustering on a folded and overtwisted thread of DNA [3, 4].

The differences in the DSB induction after irradiation with x-rays and heavy ions can be detected by fragment analysis. Production of DSBs has been conventionally studied by use of gel electrophoresis. Complementary to this indirect method, the fragment length distribution can be directly quantified by use of atomic force microscopy (AFM) [5–8].

Here we report on investigations of Ni-ion-induced DNA DSBs in an aqueous solution using the AFM technique. We present the distribution of DNA fragments induced by x-rays and Ni ions. Our results are an indication of differences in the DNA breakage pattern after photon and particle radiation.

2. Materials and methods

Intact double-stranded ΦX174 plasmid DNA (5386 bp) has been irradiated in a radioprotective aqueous buffer (20 mM HEPES) using a beam of Ni ions (3.5 MeV u^{-1}, LET = 4120 keV μm^{-1}) accelerated at the UNILAC facility at the GSI heavy ion research centre. DNA samples were irradiated as thin films of the solution (5 μl) on Petri dishes (3.5 mm diameter) with fluences of 0–4 $\times$ 10^8 part cm^{-2}. For comparison, an x-ray generator operated at 250 kV, 16 mA with 1 mm aluminium and 1 mm copper filtering was used as a conventional radiation source. The DNA samples were irradiated in Eppendorf tubes (dose range 0–3000 Gy) in anoxic conditions with a dose rate 7 Gy min^{-1}. The irradiation was performed on ice.

After irradiation, the DNA samples were diluted in a cationic solution (28.6 mM $MgCl_2$ and 50 mM KCl). A drop of 10 μl of the DNA solution was deposited on freshly cleaved mica (support medium for AFM). Atomic force microscopy of the samples was performed in a liquid environment using a self-assembled AFM operated in a contact mode. The type of induced damage was identified by differentiation of various DNA conformation forms: intact DNA was identified as supercoiled molecules; DNA damage with one single-strand break (SSB) was identified as molecules in the open circular configuration whereas occurrence of double-strand breaks (DSB) was attributed to the detection of linear molecules with two free ends. The distinguishing criteria were established in a preliminary experiment (data not shown) with control DNA samples. Biochemically prepared samples containing defined fractions of the different conformation forms were scanned and analysed to obtain the corresponding percentage values. The differentiation criteria were defined based on the comparison between the fractions calculated from AFM analysis and those known from the control sample preparations. Moreover, recorded lengths of linear fragments allow us to distinguish between molecules broken by a single DSB (this event results in a visible full length plasmid contour) or by a cluster of multiple DSBs (which produce several shorter fragments).

Based on the selected step length, the uncertainty produced by this procedure is approximately (20 nm $\approx$ 59 bp). The average number of fragments measured for each dose was at least 100. Since the longest induced fragments were of the full contour length ($\approx$1.8 μm), the AFM picture size has been chosen as 3 μm $\times$ 3 μm to assure reliable detection. On the other hand, due to a fixed number of pixels (scanning steps) of the instrument, a relatively large scan area resulted in a limited resolution. Consequently, the access to the fraction of smallest fragments has been restricted with a lower detection limit $\approx$100 nm. To achieve sufficient statistics in the analysis of fragment distribution, several samples have been scanned

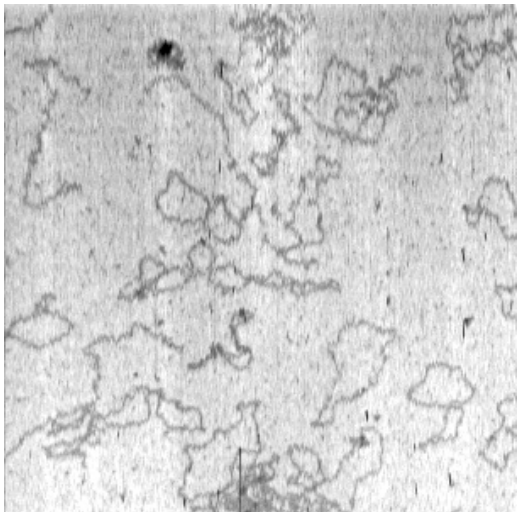

Figure 1. An exemplary contact mode AFM picture of ΦX174 DNA irradiated with Ni ions (1254 Gy) deposited on muscovite mica (3 μm × 3 μm).

for each dose. In order to compare the data obtained for heavy ions and for x-rays, the fluences Φ of particles have been transformed into corresponding doses using the formula

$$D\ (\mathrm{Gy}) = 1.6 \times 10^{-9}\ \mathrm{LET}\left(\frac{\mathrm{keV}}{\mu\mathrm{m}}\right)\Phi\left(\frac{\mathrm{part}}{\mathrm{cm}^2}\right)\frac{1}{\rho}\left(\frac{\mathrm{cm}^3}{\mathrm{g}}\right) \tag{1}$$

where $\rho = 1\ \mathrm{g\ cm}^{-3}$ is the density of the stopping material (water).

3. Results and conclusions

The measured fragment length distributions for different doses and radiation qualities (x-rays and Ni ions) have been plotted as normalized histograms to obtain the probability of producing (finding) a DNA fragment with certain length (figure 2). The figure shows that for comparable doses, heavy ions produce a considerably higher fraction of short DNA fragments than x-rays. This observation is confirmed by further analysis in terms of the average length of induced fragments as a function of the absorbed dose, obtained after using the normalized frequency histograms as probability density functions (figure 3). The average fragment length has been derived using the formula

$$\langle l \rangle = \frac{\sum_{i=1}^{n} l_i}{n} \tag{2}$$

where l_i is the length of the ith fragment and n is the number of fragments found.

Figure 3 illustrates that after ion irradiation the average length of the produced DNA fragments is systematically smaller than that for x-rays. Even for $D \to 0$ (i.e. for a single ion traversal) the average fragment length is smaller than the full plasmid contour length [8, 9].

The enhanced production of small fragments with particle radiation is in line with the concept of a particle track structure leading to an inhomogenous dose deposition in the target volume. This fact results in the locally correlated induction of DSBs through the high local doses around particle tracks. The ion-induced clustering of DSBs confirmed by direct AFM measurements appears as an excess of small- and intermediate-sized DNA fragments. This observation provides a clue for understanding the higher cell-killing efficiency of particle radiation, since multiply damaged sites on the DNA molecule are expected to reduce drastically the repair capabilities of a damaged cell.

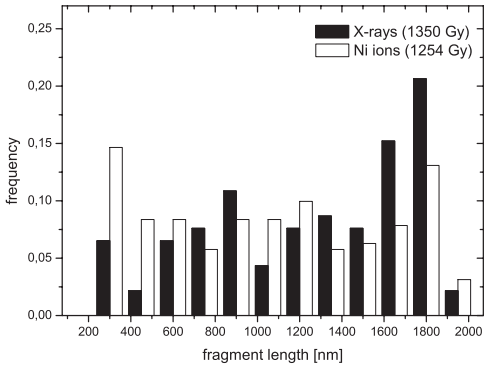

Figure 2. Measured fragment distribution of ΦX174 DNA irradiated with a dose of 1350 Gy of x-rays (black columns) and 1254 Gy of Ni ions (white columns).

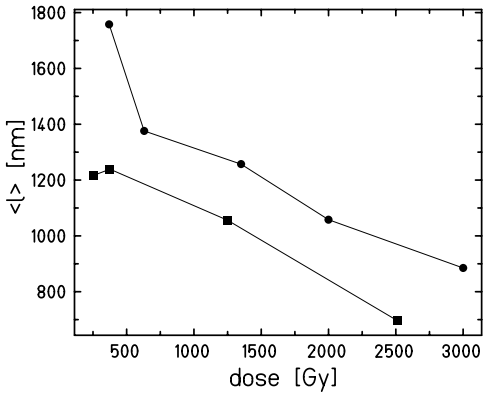

Figure 3. Comparison of the average linear fragment lengths as a function of dose: (■)—Ni ions, (●)—x-rays.

Further investigations are planned [9] to delineate the distributions and the severity of the lesions produced by irradiation with different ions and to study their relative efficiency. In addition, the understanding of the experimental data calls for further analysis using the theoretical approach based on the track structure and the radial dose distribution [10–12] and elucidation of qualitative differences between the expected and measured frequencies of fragments.

In conclusion, we have shown that AFM provides the means to analyse the plasmid DNA fragments produced by ionizing radiation with a resolution sufficient to differentiate between radiation qualities.

Acknowledgments

The authors acknowledge financial and logistic support by Professors G Kraft and R Neuman from the GSI biophysics and material science research departments.

References

[1] Alpen E L 1998 *Radiation Biophysics* (San Diego, CA: Academic)
[2] Brons S, Jakob B, Taucher-Scholz G and Kraft G 2001 *Phys. Med.* **17** 217
[3] Holley W R and Chatterjee A 1996 *Radiat. Res.* **145** 188
[4] Rydberg B 1996 *Radiat. Res.* **145** 200
[5] Hansma H G 2001 *Annu. Rev. Phys. Chem.* **52** 71
[6] Pang D, Berman B L, Chasovskikh S, Rodgers J E and Dritschilo A 1998 *Radiat. Res.* **150** 612
[7] Boichot S, Fromm M, Cunniffe S, O'Neill P, Labrune J C, Chambaudet A, Delain E and Le Cam E 2002 *Radiat. Prot. Dosim.* **99** 143
[8] Brons S, Psonka K, Heiss M, Gudowska-Nowak E and Taucher-Scholz G 2004 *Radiat. Oncol.* at press
[9] Psonka K, Brons S, Gudowska-Nowak E, Heiss M and Taucher-Scholz G 2003 *GSI Annual Report* p 158
[10] Scholz M and Kraft G 1996 *Adv. Space Res.* **18** 5
[11] Scholz M and Kraft G 2004 *Radiat. Res.* **161** 612
[12] Brons S, Taucher-Scholz G, Scholz M and Kraft G 2003 *Radiat. Environ. Biophys.* **42** 63